# Velocity Performances Indices for Parallel Mechanisms with Actuation Redundancy

Sébastien Krut, Olivier Company, François Pierrot

# Velocity performance indices for parallel mechanisms with actuation redundancy

Sébastien Krut, Olivier Company and François Pierrot

*LIRMM, UMR 5506, CNRS-UM2, 161 rue Ada, 34392 Montpellier cedex 5 (France)*
*E-mail: krut, company, pierrot@lirmm.fr*

(Received in Final Form: June 11, 2003)

## SUMMARY
This paper analyses the concept of velocity isotropy for Parallel Mechanisms with Actuation Redundancy (PMAR). The limits of classical indices based on the Jacobean matrix condition number are shown. It is proposed to use either the largest ellipsoid included in the operational polytop, or the operational polytop itself, as better representations of a PMAR capabilities. The polytop is studied because it is actually the accurate representation of a machine capability, while the largest ellipsoid remains similar to the classical tool roboticists are dealing with for decades. Velocity performance indices are proposed, and the ways to compute them efficiently are given.

KEYWORDS: Performance indices; Parallel mechanisms; Actuation redundancy; Velocity isotropy; Operational polytop.

## 1. INTRODUCTION
When designing a machine, optimization processes are often run aiming at pointing out the machine of "best performances". For this task, quality indices are used. According to the machine purpose, one index is selected, and that will lead to the machine which provides the best score, i.e. which offers the best index value. Actually, optimization is often more delicate and often ends with a compromise of several abilities because of the antagonist evolution of various abilities that are essential to the correct behavior of the mechanism.

Among all the quality indices, the Jacobian matrix condition number is often used; it is supposed to characterize the velocity isotropy of the mechanism. Due to the force-velocity duality,* it is also often said to be representative of forces isotropy. The related concept of manipulability, described as the ability to move in arbitrary directions, has been the basis of many kinematic design researches in robotics since the work of Salisbury and Craig.[1] The mathematical basics which are the foundations of the isotropy concept for robots have been first defined for serial robots,[2,3] and then more deeply investigated in, e.g. references [4–6], and it turns out that a deeper analysis is required when considering more complex mechanisms. The case of closed chain manipulator has been addressed long time ago[7] as well as more recently[8] but not unlike the open chain case. Two-arm robots, or more generally, cooperating

robot systems, have been analyzed with various approaches aiming at managing properly the capability of the complete multi-arm robot, e.g. in references [9, 10] by considering a quadratic form constructed from the Jacobians of each single arm. More recently, a unified approach has been proposed to evaluate the manipulability of closed kinematic chains[11] under a general mathematical framework using the coordinate-free methods of Riemannian geometry: this work considers all kind of closed chain robot arms, including redundant or over-actuated ones (this approach includes dynamic manipulability as well, which is out of the scope of this paper).

This paper aims at offering an analysis of isotropy concept when considering PMAR (Parallel Mechanisms with Actuation Redundancy), i.e. parallel mechanisms where a given operational force does not correspond to a unique set of joint forces. This type of redundancy differs from the kinematic redundancy (cf. Figure 1) case where a given operational velocity does not correspond to a unique set of joint velocities. It has been shown[12,13] that actuation redundancy may help to overcome the problem of over-mobility singularities, and it seems important to offer tools to correctly analyze the velocity performances of such machines. The case of such mechanisms has been partially addressed in reference [14] where the problem of "internal" forces is taken into account to derive a task space polytop.

In Section 2, some basic issues related to the use of the Jacobian condition number as a manipulability measure are firstly recalled and one of its important limitations is pointed out when considering PMAR: this index does not provide a proper measure of kinematic isotropy when this term means "ability to perform the same speed along different directions" (Figure 2). Section 3 is dedicated to the definition of a representation of isotropy which is consistent with the well known condition number since it refers to measures made on a velocity ellipsoid; however, the ellipsoid that must be considered is rather different from the usual one. Two different algorithms are given: one is based on derivations made in joint space, and the other one on derivations made in operational space. Section 4 is a discussion about different possible indices and the relevant algorithms: they are based on an analysis of the velocity polytop.

Indeed, parallel machines with actuation redundancy have already been built,[12–16] and the time has come for the definition of design and analysis tools which can properly
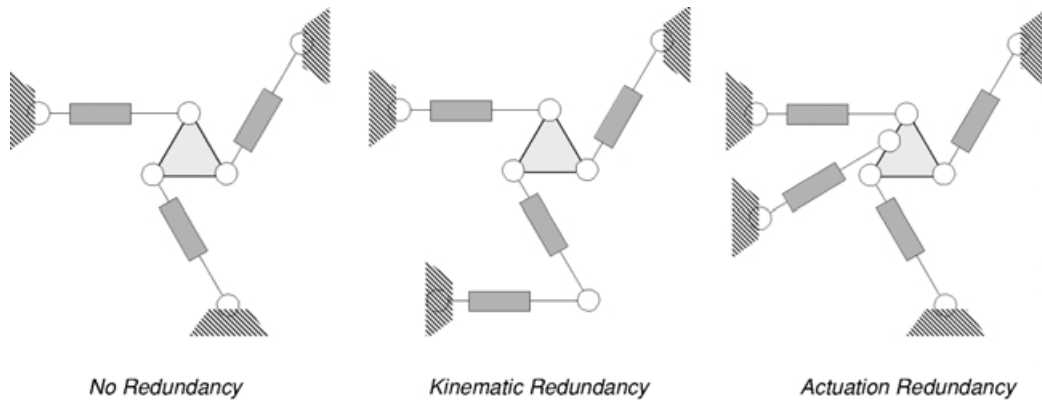
---

* See our analysis of the "velocity-force duality" in Section 2–3.

No Redundancy          Kinematic Redundancy          Actuation Redundancy

Fig. 1. A planar PKM and different type of redundancy.

deal with such machines. This paper is a step towards this goal.

## 2. CONDITION NUMBER AND ITS APPLICATION TO PMAR

In the following a mechanism is characterized by its inverse Jacobian, $\mathbf{J_m}$, which links joints velocities $\dot{\mathbf{q}}$ to operational speed, $\dot{\mathbf{x}}$, as follows:†

$$\dot{\mathbf{q}} = \mathbf{J_m}\dot{\mathbf{x}} \tag{1}$$

### 2.1 Is a Two-dof X-Y Table an Isotropic Device?

In order to illustrate the following discussion, let us consider the simple case of a serial 2-dof X-Y table in Figure 3.

For this mechanism, $\mathbf{J_m}$ is the identity matrix, and for the robotics community, this mechanism is often considered as perfectly isotropic; velocity performances are said to be identical in all directions of the operational space. This is clearly not true, as shown in Figure 4 and Figure 5.

Reachable joint velocity space is actually a square defined by $|\dot{q}_i| \leq \dot{q}^{max}$. This square remains a square once mapped in the operational space using matrix $\mathbf{J_m}^{-1}$. Therefore the highest velocity reachable by the moving platform is $v^{max} = \sqrt{2} \times \dot{q}^{max}$. Such a speed is only accessible for a very specific motion direction, while $v^{min} = \dot{q}^{max}$ is

† The notation $\dot{\mathbf{x}}$ does not mean it is the derivative of operational vector with respect to time.

reachable for all operational directions. Graphically, this results in the circle of radius $v^{min}$ inscribed in the square. This circle is the image of the joint space circle of radius $\dot{q}^{max}$ by the linear mapping represented by matrix $\mathbf{J_m}^{-1}$. Interestingly enough, even if this is not an isotropic device strictly speaking (in the sense of "same velocity along different directions"), roboticists consider it as a perfectly isotropic design for the following reason: there is no deformation of the velocity joint space circle (or hyper-sphere for higher orders) by the Jacobian matrix. Stated another way, classical techniques consider the manipul-ability as a measure of the "quality" of the velocity *mapping* (from joint space to task space), and it turns out it is often closely related to the isotropy of the machine itself.

### 2.2 Analysis of a Basic Non-redundant Parallel Mechanism

The simple parallel mechanism in Figure 6 is made of two connecting rods linking two identical linear motors to the moving platform. Obviously, the moving platform can move in translation along two directions.

The inverse Jacobian matrix of this mechanism in this centered position is the same as for the X-Y table (joint and operational reachable domains are those represented in Figure 4 and Figure 5). When the mechanism is not in its centered position, the inverse Jacobian matrix is not equal to the identity matrix anymore; so if the reachable joint
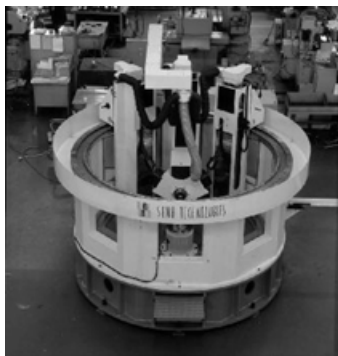


Eclipse: a PMAR at the
University of Seoul
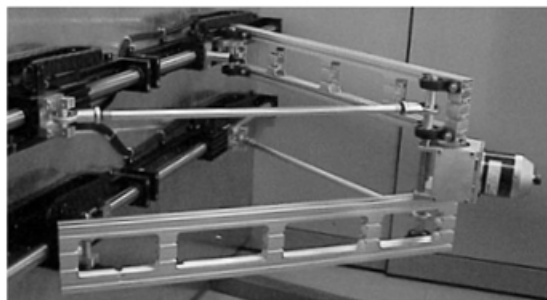
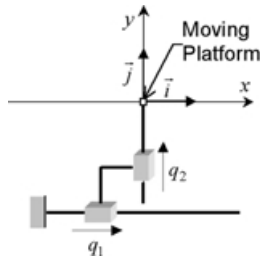Archi: a PMAR at the LIRMM

Fig. 2. Existing PMAR.

Fig. 3. X-Y table geometry.

domain remains the same, the reachable operational domain becomes a polytop (see Figure 7).

The image of the joint circle is an ellipse inscribed in the polytop. This ellipse is entirely characterized by the SVD‡
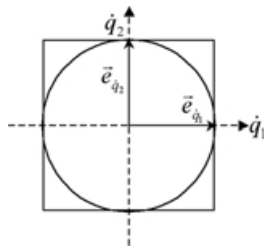


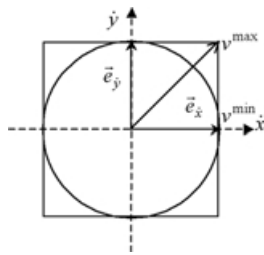Fig. 4. Reachable joint space of the X-Y table.



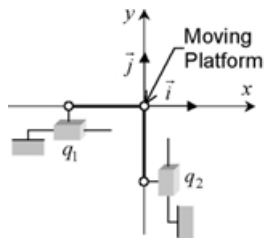Fig. 5. Reachable velocity operational space of the X-Y table.
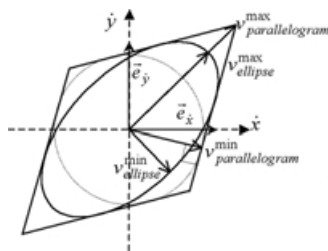


Fig. 6. V-shape Parallel Mechanism Geometry.



Fig. 7. Reachable operational space for a simple parallel mechanism.
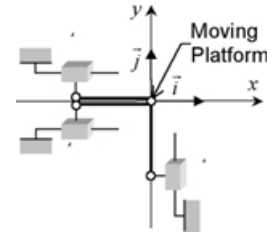
‡ Singular Value Decomposition.



Fig. 8. Geometry of a specific PMAR.

of $\mathbf{J_m}$; the SVD provides in particular the lengths of the ellipse's axes. A usual isotropy index is derived as the ratio of extreme operational velocities: $v_{ellipse}^{max}$ and $v_{ellipse}^{min}$; this index is a measure of the ellipse's distortion. The lower the distortion is (index value close to 1), the more the ellipse tends towards the circle, considered as an "ideal case" from the isotropy point of view.

Rather than considering the ellipse, one could be interested in the more realistic polytop that may be analyzed in terms of ratio between the absolute maximal speed ($v_{parallelogram}^{max}$) and the maximum speed that the mechanism can reach in all operational space directions ($v_{parallelogram}^{min}$). The latter graphically corresponds to the radius of the largest circle inscribed in the operational polytop.

In this paper, discussions related to PMAR are made for both cases, velocity ellipsoid and velocity polytop; however, the usual inverse Jacobian matrix condition number cannot be used straightforward, as shown in the next section.

### 2.3 A Basic PMAR – 3 Actuators/2 dof

Let us consider the PMAR in Figure 8, made up of three connecting rods and three identical linear actuators. Here, two actuators are collinear which means that two connecting rods are collinear as well. This really specific case is used here as a trivial example showing clearly the limits of classical derivations.

In the central position of Figure 8, the actuated chain (joint position: $q_3$) added to the mechanism of Figure 6 is exactly in the same situation than the chain No. 1. This mechanism produces in term of velocities the same effects that the former non-redundant parallel mechanism (Figure 6). So, in this central position, this mechanism is as isotropic from the velocity point of view as the previous mechanism or even the X-Y table; operational velocities explore the same field as previously: the operational polytop is a square (Figure 5).

The inverse Jacobian matrix of this PMAR, $\mathbf{J_m}$, is given by:

$$\mathbf{J_m} = \begin{bmatrix} 1 & 0 \\ 0 & 1 \\ 1 & 0 \end{bmatrix} \tag{2}$$

and its condition number, defined as the ratio of the maximum and minimum singular values of $\mathbf{J_m}$, is equal to $\sqrt{2}$. Thus, the ratio between extreme singular values does not represent anymore the ratio of extreme dimensions of the ellipse of *maximum* surface inscribed in the operational polytop, since this ratio should be equal to 1. Indeed, the operational ellipse obtained using the SVD has two half-
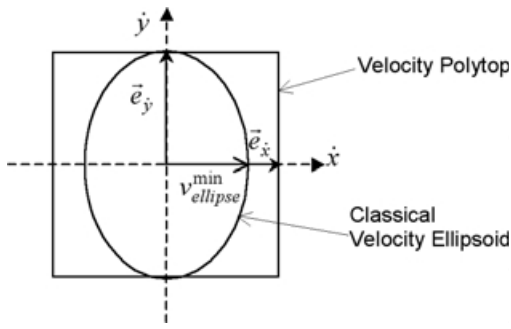
Fig. 9. Reachable operational space for this specific PMAR.

axes which length are $\dot{q}_{max}$ and $\dot{q}_{max}/\sqrt{2}$ as depicted in Figure 9.

In other words, the usual isotropy index says such a machine is far from being isotropic, when a common sense analysis says it is as isotropic as an X-Y table. Indeed, in such cases, the condition number may give a rough estimate of the anisotropy in force (in reality the machine maximum force along *x* is twice the maximum force along *y*), but it does not represent anything related to the machine velocity isotropy.

Even in the approach proposed by Park et al.[11] the matrix whose eigenvalues and eigenvectors describe the manipulability** is $\mathbf{M} = \mathbf{diag}(1/2\ 1)$; again, this matrix does not correspond to an isotropic design in the classical sense.

This situation seems rather contradictory: the machine described in Figure 8 offers the same velocity along *x* and *y* axes, while known manipulability indexes state it is not an isotropic design. For the indexes based on the Jacobian itself, the reason for that "contradiction" is clear; indeed, for PMAR the "duality" between force and velocity does not hold anymore for this simple fact: a set of joint forces can be chosen freely within the actuators capacity boundaries, while the components of the joint velocities vector must respect kinematic constraints and thus cannot be chosen freely; there is no such information embedded in the Jacobian matrix. The case of Park et al.'s approach, which offers a unified frame for the analysis of all manipulators, presents an additional subtlety: consistently with former definitions of manipulability, a manipulator is said to be in an *isotropic posture* when the forward kinematic *map* is an *isometry*.[5,11] This paper proposes a different approach by focusing on the machine actual capabilities in task space more than on the velocity mapping.

*In order to be consistent with the interpretation of the condition number established for non-redundant mechanisms, it is proposed in this paper to use the largest ellipse included in the operational polytop, rather than the ellipse given by the straightforward use of the Jacobian; Section 3 is revisiting the concept of velocity isotropy and will show how convenient this "largest" ellipse could be. An alternate solution is to resort on the operational polytop itself because it describes exactly the velocity capabilities of a given machine, and this is addressed in Section 5 as well. Selecting among these two options is let at the designer appreciation: indeed, the polytop will give the designer*

** See appendix for few details regarding this approach.

*information about the extreme cases, while the ellipse will offer a more global view of the mechanism behavior.*

## 3. REVISITING THE CONCEPT OF VELOCITY ISOTROPY FOR PMAR

### 3.1 Preliminary Remarks

– To be simple, different domains of space will be named *circle*, *ellipse*, *polytop*, *square*, *cube*. One should keep in mind that those terms must be generalized when considering spaces whose dimensions are higher than 2 or 3 (hyper-circle, hyper-ellipse, and so on).
– Only a-dimensional problems are considered here. In other cases, weighting matrices, $\mathbf{W}_{\dot{x}}$ and $\mathbf{W}_{\dot{q}}$, can be used as follows:[17]

$$\mathbf{W}_{\dot{x}} = \begin{bmatrix} 1/\dot{x}_1^{max} & & 0 \\ & \ddots & \\ 0 & & 1/\dot{x}_n^{max} \end{bmatrix}, \tilde{\mathbf{x}} = \mathbf{W}_{\dot{x}}\ \dot{\mathbf{x}}, |\tilde{\dot{x}}_i| \le 1, \quad (3)$$

$$\mathbf{W}_{\dot{q}} = \begin{bmatrix} 1/\dot{q}_1^{max} & & 0 \\ & \ddots & \\ 0 & & 1/\dot{q}_n^{max} \end{bmatrix}, \tilde{\mathbf{q}} = \mathbf{W}_{\dot{q}}\ \dot{\mathbf{q}}, |\tilde{\dot{q}}_i| \le 1, \quad (4)$$

Weighting matrices help in managing issues such as: non-homogeneity (coexistence of linear and angular velocities), differences in actuators' performances ($\dot{q}_i^{max} \ne \dot{q}_j^{max}$), differences in desired performances along various operational axes ($\dot{x}_i^{max} \ne \dot{x}_j^{max}$).

### 3.2 Analysis of the SVD for a Redundant Mechanism

For illustration purpose the planar mechanism shown in Figure 10 will be used here. It is a 3-actuator-2-dof PMAR, which geometry is more general than the one in Section 2.3. However, formulas will be established for any type of joint and operational spaces, as long as they respect the following condition:

$$m > n, \text{ with } \dim(\dot{\mathbf{q}}) = m \text{ and } \dim(\dot{\mathbf{x}}) = n \quad (5)$$

The SVD of the inverse Jacobian matrix gives[18]:

$$\mathbf{J_m} = \mathbf{U}\ \mathbf{S}\ \mathbf{V^T} \quad (6)$$

where:

– $\mathbf{V^T}$ is a $n \times n$ orthogonal matrix, representing a linear application in the operational space;
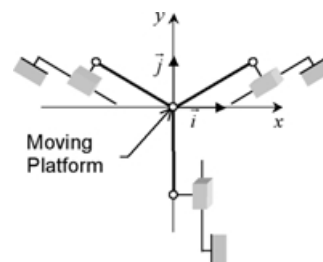


Fig. 10. Geometry of a typical parallel redundant mechanism.

– **S** is a rectangular matrix whose upper part includes the singular values of, $\mathbf{J_m}$, $\sigma_1$, ⋯, $\sigma_n$:

$$\mathbf{S} = \begin{bmatrix} \sigma_1 & & 0 \\ & \ddots & \\ 0 & & \sigma_n \\ & 0 & \end{bmatrix} \begin{matrix} \\ n \\ \\ \end{matrix} \Bigg| m \qquad (7)$$

It characterizes the linear application that links a operational velocity vector to a joint velocity vector.

– **U** is a $m \times m$ orthogonal matrix, representing a linear application in the joint space. The $n$ first columns, vectors $U_1, \ldots, U_n$ ($n < m$) span the range of $\mathbf{J_m}$. The $m - n$ following columns correspond to the actuators velocities which can never be produced by a movement of the moving platform. They span the kernel of $\mathbf{J_m}$.

$$\mathbf{U} = \begin{bmatrix} U_1 \ldots U_n \vdots \end{bmatrix} m \qquad (8)$$

To be acceptable, i.e. to be admissible by the mechanism, a joint velocity vector must belong to the range of $\mathbf{J_m}$. Let us note (Figure 11):

– $\{\vec{e}_{\dot{Q}_1}, \ldots, \vec{e}_{\dot{Q}_n}\}$, a base for this type of vector;
– **Q** ($\dim(\mathbf{Q})=n$), a column matrix representative of the joint velocity vecor in this base;
– $\mathbf{S_1}$, a matrix representing a mapping from the operational space to the restriction of the joint space to the range of $\mathbf{J_m}$:

$$\mathbf{S_1} = \begin{bmatrix} \sigma_1 & & 0 \\ & \ddots & \\ 0 & & \sigma_n \end{bmatrix} n \qquad (9)$$

The following equation links an admissible joint velocity vector to an operational velocity vector:

$$\dot{\mathbf{x}} = \mathbf{V} \ \mathbf{S_1}^{-1} \ \tilde{\mathbf{Q}} \qquad (10)$$

The restriction of the unit sphere to the range of $\mathbf{J_m}$ is a circle of radius 1 (cf. Figure 12). This circle is transformed into an ellipse in the operational space; the ellipse's half-
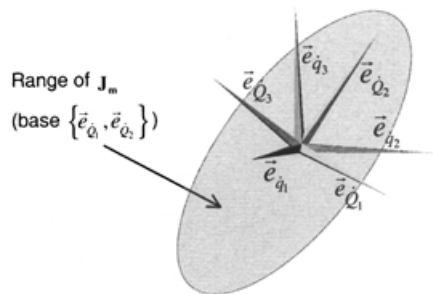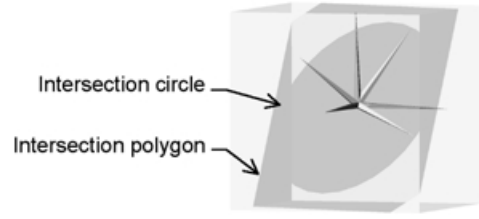


Fig. 12. Intersection of the unit cube and the unit sphere with the range of $\mathbf{J_m}$.

axes length are $1/\sigma_i$, $i \in \{1, \ldots, n\}$. The condition number of $\mathbf{J_m}$ is an image of this ellipse's shape.

Obviously, the entire acceptable joint space is not a sphere but a cube defined by the following inequalities:

$$-1 \le \dot{q}_i \le 1, i \in \{1, \ldots, m\} \qquad (11)$$

The restriction of this cube to the range of $\mathbf{J_m}$ (cf. Figure 12) is a polygon, or polytop. All acceptable actuator velocity vectors must be located inside this polygon. In Figure 13, the circle and the polygon are depicted. It is to be noted that the circle could be larger and still acceptable because it is not tangent with the polygon. *That implies that the opposite of the singular values are not enlightening maximum speeds which can be reached by the moving platform.*

For a non-redundant mechanism, the joint circle and the operational ellipse are the greatest ellipses respectively included into the joint square and the operational polytop; for a PMAR, this is no more the case (cf. Figure 14 and Figure 15).

*It is proposed in this paper to consider the largest ellipse included in the operational polytop. The ratio of the extreme half-axes of this ellipse can be a more significant isotropy index. Furthermore, it is proposed as well to consider another index constituted by the ratio between the extreme velocities measured at the polytop level, $v_{polytop}^{max}$ and $v_{polytop}^{min}$.*
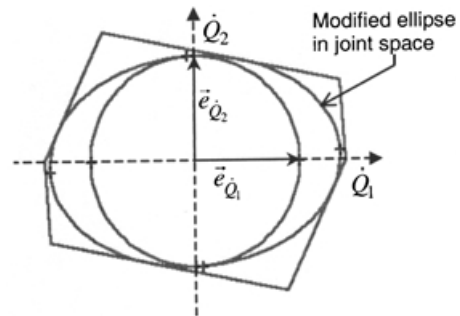


Fig. 13. Joint polygon and circle.



Fig. 11. Graphical representation of $\dot{\mathbf{q}} = \mathbf{U} \ \dot{\mathbf{Q}}$.



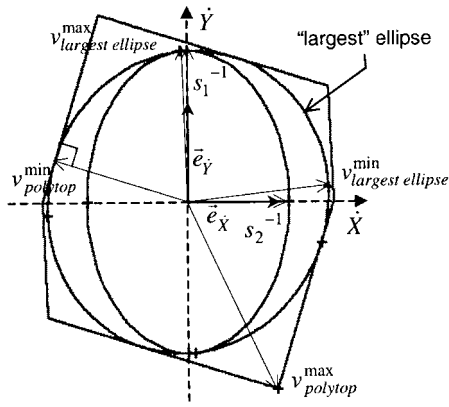Fig. 14. Joint velocities for a PMAR.

Fig. 15. Operational velocities for a PMAR.

### 3.3 Case Study

The complete situation is depicted in Figure 16 for a given geometry [120° between each actuator, length of arms = 100, position of the moving platform ($-40$, $-10$)].

The obtained results are given in Table I. The modified operational ellipse is clearly a better representation of the machine velocity capability than the ellipse associated with the restriction of joint space unit sphere (operational ellipse in Figure 14).

*The purposes of Section 3 were mainly:*

– *to point out the limits of the classical definition of the isotropy ellipsoid when dealing with PMAR;*
– *to propose the use of either the largest ellipse included in the operational polytop, or the operational polytop itself, as better representations of a PMAR velocity capabilities.*
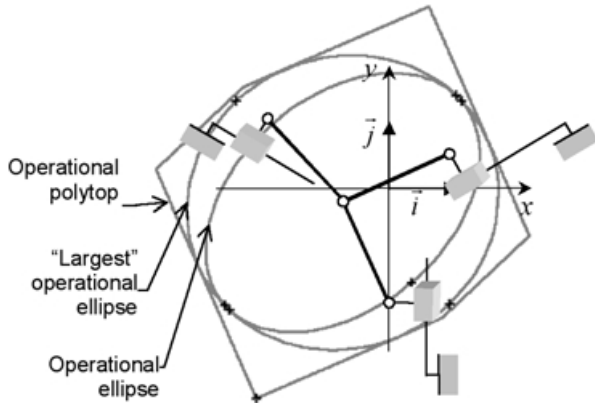


Fig. 16. Operational velocity situation centered on the moving platform.

Table I. Results and indices values.

| | |
|---|---|
| $cond(\mathbf{J_m})$ | 1.49 |
| "Largest" ellipse index | 1.08 |
| $v_{modified\ ellipse}^{max}$ | $1.35 \times \dot{q}_{max}$ |
| $v_{modified\ ellipse}^{min}$ | $0.97 \times \dot{q}_{max}$ |
| Polytop index | 1.48 |

*The paper now addresses ways to establish the largest ellipsoid and the polytop.*

## 4. SEARCH OF THE OPERATIONAL ELLIPSE OF GREATEST SURFACE INCLUDED INTO THE ADMISSIBLE OPERATIONAL POLYTOP

This search can be made:

– by reasoning in joint space, i.e. finding the largest ellipse in joint space and then mapping it into the operational space (Section 4.1);
– by reasoning directly in the operational space (Section 4.2). It will be shown that the resulting ellipses are actually identical.

### 4.1 Reasoning in Joint Space

The application which transforms the joint unitary circle of the subspace image of $\mathbf{J_m}$ into the joint ellipse of largest surface included in the joint polytop will be determined here. This ellipse, once mapped into the operational space by the linear application of matrix $\mathbf{S}_1^{-1}$ gives the ellipse of largest surface included into the operational polytop (this point will be proved in the next section). The conditions which must be respected by the joint ellipse to be located inside the joint polytop will be firstly presented; then the conditions to find the largest ellipse will be formulated as an optimization problem.

**4.1.1 General Approach.** Let $M$ be a point of the range of $\mathbf{J_m}$ and belonging to the unitary circle. Vector $\overrightarrow{OM}$ (where $O$ is the origin of the frame) is a linear combination of vectors $\vec{e}_{\dot{Q}_i}, \ldots, \vec{e}_{\dot{Q}_n}$. Let $\mathbf{M}$ be the column matrix representative of this vector in the base of the range $B_{Im(\mathbf{J_m})} = (\vec{e}_{\dot{Q}_i}, \ldots, \vec{e}_{\dot{Q}_n})$. The relation $\|\overrightarrow{OM}\| = 1$ results in:

$$\mathbf{M^T}, \mathbf{M} = 1 \qquad (12)$$

The largest ellipse in joint space is calculated with two transformations: (i) the original unitary circle is expanded (point $M$ is transformed in point $\tilde{M}$); (ii) the expanded ellipse is rotated (point $\tilde{M}$ is transformed in point in $M'$). Thus (Figure 17):

– $\tilde{M}$ belongs to an ellipse whose axes are the vectors of $B_{Im(\mathbf{J_m})}$, and whose half-axes length are $d_1, \ldots, d_n$. The column matrix representative of point $\tilde{M}$ in frame of origin $O$ and base $B_{Im(\mathbf{J_m})}$, is noted $\tilde{\mathbf{M}}$, and verifies:

$$\tilde{\mathbf{M}} = \mathbf{D}, \mathbf{M} \qquad (13)$$

where $\mathbf{D} = diag(d_1, \ldots, d_n)$.

– $M'$ belongs to the ellipse of greatest surface. $\mathbf{M'}$, the matrix associated to point $M'$ verifies:

$$\mathbf{M'} = \mathbf{R}, \tilde{\mathbf{M}} \qquad (14)$$

with $\mathbf{R}$ an orthogonal matrix.

Expansion and orientation are combined to get the largest ellipse. To be included in the joint polytop, the ellipse must verify:

– the ellipse is located inside the unitary cube,
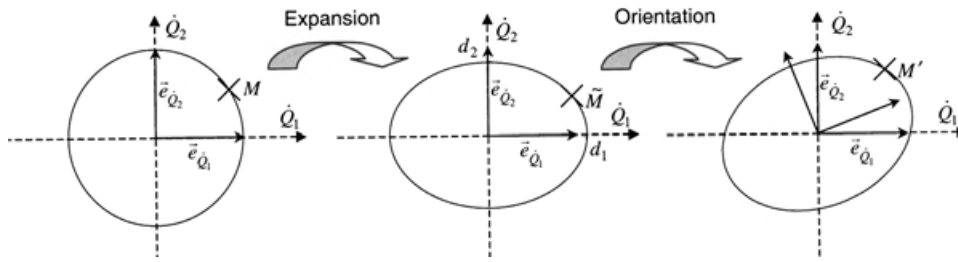– it belongs to the range of $\mathbf{J_m}$ (true by construction).

Fig. 17. From the unitary circle to the largest ellipse.

To belong to the joint cube, point $M'$ must respect the following condition:

$$\vec{e}_{\dot{q}_i} \cdot \overrightarrow{OM'} \le 1 \quad i = 1, \dots, m \tag{15}$$

Indeed, the cube is defined by $2m$ faces. However, the problem is symmetric with respect to point $O$, and only $m$ faces have to be considered. Such faces are directed by vectors $\vec{e}_{\dot{q}_i}$, $i \in \{1, \dots, m\}$, of the joint space canonic base. This expresses the fact that $M'$ belongs to the $i$th admissible domain of space, delimited by the plane perpendicular to $\vec{e}_{\dot{q}_i}$, such that the distance from point $O$ to the plane is equal to 1. This can be written in matrix form as follows:

$$\mathbf{E_i^T}\ \mathbf{M'} \le 1 \tag{16}$$

where $\mathbf{E_i}$ is the column matrix associated to vector $\vec{e}_{\dot{q}_i}$ in base $B_{Im(J_m)} = (\vec{e}_{\dot{Q}_1}, \dots, \vec{e}_{\dot{Q}_n})$.

**4.1.2 Finding the Vectors Perpendicular to the Ellipse and the Polytop.** To guarantee that all ellipse points belong to the $i$th admissible domain, it is sufficient to verify that the point closest to the $i$th face is inside this domain. For such a point, the vector $\vec{n}'$ perpendicular to the ellipse, is collinear to the vector $\vec{e}'_{\dot{q}_i}$, perpendicular to the considered face of the polytop (cf. Figure 18).

Let $\vec{e}'_{\dot{q}_i}$ be the projection of vector $\vec{e}_{\dot{q}_i}$ in the range of $\mathbf{J_m}$. Because $B_{Im(J_m)}$ does only direct a subpart of the articular space it has to be noticed that $\mathbf{E_i}$ is also the column matrix associated to vector $\vec{e}'_{\dot{q}_i}$.

The colinearity relationship is expressed as:

$$\exists k / \mathbf{N'} = k \times \mathbf{E_i} \tag{17}$$

where:

– $\mathbf{N'}$ is the column matrix associated to vector $\vec{n}$ in base $B_{Im(J_m)}$,
– $\mathbf{E_i}$ is the column matrix associated to vector $\vec{e}'_{\dot{q}_i}$.

Let point $\tilde{M}$ be defined in the frame $\langle O, B_{Im(J_m)}\rangle$ by the following set of coordinates: $(x_1, \dots, x_n)$. Then the ellipse
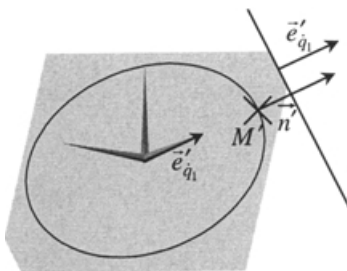


Fig. 18. Colinearity normal to the ellipse/normal to the frontier.

whose axis are the vectors of $B_{Im(J_m)}$, and whose half-axes length are $d_1, \dots, d_n$ is defined by:

$$f(\tilde{M}) = \frac{x_1^2}{d_1^2} + \dots + \frac{x_n^2}{d_n^2} - 1 = 0 \tag{18}$$

And the vector perpendicular to the ellipse at point $\tilde{M}$, $\vec{n}$, is defined by:

$$\vec{n} = [\overrightarrow{grad}\ f](\tilde{M}) = \frac{2x_1}{d_1^2}\vec{e}_{\dot{Q}_1} + \dots + \frac{2x_n}{d_n^2}\vec{e}_{\dot{Q}_n}. \tag{19}$$

With matrix in base $B_{Im(J_m)}$, this results in relation:

$$\tilde{\mathbf{N}} = \mathbf{D}^{-2}\tilde{\mathbf{M}} \tag{20}$$

In fact, because $\mathbf{D}$ is a diagonal matrix, $\mathbf{D}^{-2}$ is defined by:

$$\mathbf{D}^{-2} = \begin{bmatrix} 1/d_1^2 & & 0 \\ & \ddots & \\ 0 & & 1/d_n^2 \end{bmatrix}. \tag{21}$$

Then $\vec{n}'$ is obtained as:

$$\mathbf{N'} = \mathbf{R}\,\tilde{\mathbf{N}}. \tag{22}$$

with $\mathbf{R}$ a rotation matrix.

**4.1.3 Defining the Admissible Ellipses.** To summarize the situation, the system of matrix equations to be solved is the following:

$$\forall i \in \{1, \dots, m\}, \begin{cases} \mathbf{M^T M} = 1 & (12) \\ \tilde{\mathbf{M}} = \mathbf{D M} & (13) \\ \mathbf{M'} = \mathbf{R}\,\tilde{\mathbf{M}} & (14) \\ \mathbf{E_i^T M'} \le 1 & (16) \\ \exists k / \mathbf{N'} = k \times \mathbf{E_i} & (17) \\ \tilde{\mathbf{N}} = \mathbf{D}^{-2}\tilde{\mathbf{M}} & (20) \\ \mathbf{N'} = \mathbf{R}\,\tilde{\mathbf{N}} & (22) \end{cases}$$

Equations (13) and (14) imply that:

$$\mathbf{M'} = \mathbf{R D M}. \tag{23}$$

Equations (20) and (22) lead to:

$$\mathbf{N'} = \mathbf{R D}^{-2}\tilde{\mathbf{M}}, \tag{24}$$

Equations (24) and (13) lead to:

$$\mathbf{N'} = \mathbf{R D}^{-1}\mathbf{M}. \tag{25}$$

Inverting Equation (25) leads to:

$$\mathbf{M} = \mathbf{D}\,\mathbf{R^T}\,\mathbf{N'}. \tag{26}$$

Combining Equations (23) and (16) gives:

$$\mathbf{E_i^T}\,\mathbf{R}\,\mathbf{D}\,\mathbf{M} \le 1, \tag{27}$$

combining Equations (17) and (26) gives:

$$\exists k/\ \mathbf{M} = k \times \mathbf{D}\,\mathbf{R^T}\,\mathbf{E_i}, \tag{28}$$

combining Equations (28) and (12), knowing that $\mathbf{D}$ is diagonal, can be written as follows:

$$\exists k/k^2\,\mathbf{E_i^T}\,\mathbf{R}\,\mathbf{D^2}\,\mathbf{R^T}\,\mathbf{E_i} = 1. \tag{29}$$

In the same way, combining Equations (28) and (16) leads to:

$$\exists k/k\,\mathbf{E_i^T}\,\mathbf{R}\,\mathbf{D^2}\,\mathbf{R^T}\,\mathbf{E_i} \le 1. \tag{30}$$

While making sure that $0 \le k\,\mathbf{E_i^T}\,\mathbf{R}\,\mathbf{D^2}\,\mathbf{R^T}\,\mathbf{E_i}$, Equation (30) gives:

$$\exists k/k^2\mathbf{E_i^T}\,\mathbf{R}\,\mathbf{D^2}\,\mathbf{R^T}\,\mathbf{E_i} \times \mathbf{E_i^T}\,\mathbf{R}\,\mathbf{D^2}\,\mathbf{R^T}\,\mathbf{E_i} \le 1. \tag{31}$$

Knowing Equation (29), (31) simplifies in the inequality:

$$\mathbf{E_i^T}\,\boldsymbol{\Sigma}\,\mathbf{E_i} \le 1, \tag{32}$$

with $\boldsymbol{\Sigma} = \mathbf{R}\,\mathbf{D^2}\,\mathbf{R^T}$, a symmetrical matrix.

*Of course, Equation (32) has to be verified for all $i = 1, \ldots, m$.*

As a matter of fact, a relation exists between vectors $\mathbf{E_i}$ and matrix $\mathbf{U}$. Matrix $\mathbf{U}$ can be expressed as follows:

$$\mathbf{U} = [\mathbf{U_1} \,|\, \mathbf{U_2}] \tag{33}$$

with:

$$\mathbf{U_1} = \begin{bmatrix} \vec{e}_{\dot{q}_1} \cdot \vec{e}_{\dot{Q}_1} & \ldots & \vec{e}_{\dot{q}_1} \cdot \vec{e}_{\dot{Q}_n} \\ & \ldots & \\ \vec{e}_{\dot{q}_n} \cdot \vec{e}_{\dot{Q}_1} & \ldots & \vec{e}_{\dot{q}_m} \cdot \vec{e}_{\dot{Q}_n} \end{bmatrix},$$

$$\mathbf{U_2} = \begin{bmatrix} \vec{e}_{\dot{q}_1} \cdot \vec{e}_{\dot{Q}_{n+1}} & \ldots & \vec{e}_{\dot{q}_1} \cdot \vec{e}_{\dot{Q}_m} \\ & & \\ \vec{e}_{\dot{q}_m} \cdot \vec{e}_{\dot{Q}_{n+1}} & \ldots & \vec{e}_{\dot{q}_m} \cdot \vec{e}_{\dot{Q}_m} \end{bmatrix}. \tag{34}$$

And since $\mathbf{E_i} = \begin{bmatrix} \vec{e}_{\dot{q}_i} \cdot \vec{e}_{\dot{Q}_1} \\ \vdots \\ \vec{e}_{\dot{q}_i} \cdot \vec{e}_{\dot{Q}_n} \end{bmatrix}$ $\mathbf{U_1}$ is expressed as follows:

$$\mathbf{U_1} = \begin{bmatrix} \mathbf{E_1^T} \\ \vdots \\ \mathbf{E_m^T} \end{bmatrix} \tag{35}$$

Noting $\mathbf{U_1}(i)$ the $i$th line of matrix $\mathbf{U_1}$ Equation (20) can be rewritten as:

$$\forall i \in \{1, \ldots, m\}\ \mathbf{U_1}(i)\,\boldsymbol{\Sigma}\,\mathbf{U_1}(i)^T \le 1. \tag{36}$$

**4.1.1 Finding the Largest Admissible Ellipse.** Among all those ellipses respecting Equation (35), the one of maximal surface still have to be found. This problem is described here as an optimization problem.

The surface of an hyper-ellipse equals to:

$$A = k \times \prod_{i=1}^{n} d_i, \tag{37}$$

with $k = \pi$ for $n = 2$, $k = (4/3)\pi$ for $n = 3$, etc.

Maximizing $A$ is equivalent to maximizing the product of the ellipse half-axes length. It is also equivalent to minimizing the following expression: $-\prod_{i=1}^{n} d_i^2$.

It can be seen that the determinant of $\mathbf{S}$ is:

$$\det(\boldsymbol{\Sigma}) = \det(\mathbf{R}) \times \det(\mathbf{D^2}) \times \det(\mathbf{R^{-1}}) = \det(\mathbf{D^2}), \tag{38}$$

so:

$$\det(\boldsymbol{\Sigma}) = \prod_{i=1}^{n} d_i^2 \tag{39}$$

> To conclude, determining the ellipse of greatest surface included in the joint polytop, consists in finding the *symmetrical* matrix $\boldsymbol{\Sigma}$ which verifies:
>
> $$-\det(\boldsymbol{\Sigma})\ \text{minimum}$$
>
> $$\text{under constraints}$$
>
> $$\mathbf{U_1}(i)\,\boldsymbol{\Sigma}\,\mathbf{U_1}(i)^T \le 1\ \ \forall i \in \{1, \ldots, m\}.$$

The eigenvalue decomposition of the *real symmetric* $\boldsymbol{\Sigma}$ gives:

$$\boldsymbol{\Sigma} = \mathbf{R}\,\boldsymbol{\Delta}\,\mathbf{R^T}, \tag{40}$$

with:

– $\mathbf{R}$ is the orientation matrix (note that $\mathbf{R^T} = \mathbf{R^{-1}}$),

– $\boldsymbol{\Delta} = \mathbf{diag}(\delta_1, \ldots, \delta_n)$,

– $d_i = \sqrt{\delta_i}$.

The knowledge of $\mathbf{R}$ and $\mathbf{D}$ characterizes entirely the ellipse of greatest surface included inside the joint polytop. This matrix is then mapped by matrix $\mathbf{S_1^{-1}}$ to the ellipse of largest surface included in the operational polytop (this point will be proven in next section).

*The sought matrix which represents the transformation of a unitary circle in the admissible part of joint space into the largest ellipse included inside the operational space polytop is given by:*

$$\mathbf{X} = \mathbf{S_1^{-1}}\mathbf{R}\mathbf{D} \tag{41}$$

*The indices we recommend to use are then related to singular values of **this** matrix, e.g. cond($\mathbf{X}$), or $\min(\sigma(\mathbf{X}))$, etc.*

### 4.2 Reasoning in Operational Space

The reasoning of Section 3.3.1 has been conducted in joint space; however, rather than seeking the ellipse of maximum surface included inside the joint polytop, and then computing its image in the operational space, it is possible to find the ellipse of greatest surface included inside the operational polytop. The following relation describes the mapping between the operational space and the range of $\mathbf{J_m}$:

$$\mathbf{M'} = \mathbf{S_1}\ \mathbf{K'}, \tag{42}$$

with:

– $M' \in range(\mathbf{J_m})$,
– $K'$ a point in operational space,
– $\mathbf{M'}$ the column matrix associated with $M'$ in $\mathbf{B}_{\mathrm{Im}(\mathbf{J_m})}$,
– $\mathbf{K'}$ the column matrix associated with $K'$ in the singular vectors base.

$M'$ belongs to the joint polytop:

$$\mathbf{E_i^T M'} \leq 1 \quad i = 1, \ldots, m. \tag{43}$$

Thanks to relation (42), Equation (43) becomes in operational space:

$$\mathbf{E_i^T S_1 K'} \leq 1. \tag{44}$$

Since Equation (44) is the only equation that differs from the system of equations of the previous section, the resolution of the system leads to:

$$\forall i \in \{1, \ldots, m\} \ \mathbf{U_1}(i) \mathbf{S_1} \mathbf{\Sigma'} \mathbf{S_1^T} \mathbf{U_1}(i)^{\mathrm{T}} \leq 1, \tag{45}$$

where $\mathbf{\Sigma'}$ is a symmetrical matrix defined as follows:

$$\mathbf{\Sigma'} = \mathbf{R'D'^2 R'^T} \tag{46}$$

Those equations express the constraints that must be fulfilled by the operational ellipse to be located inside the operational polytop. Those relations are very similar to those obtained in the joint space.

In the operational space, the optimization problem consists in finding a *symmetrical* matrix $\mathbf{\Sigma'}$ which verifies:

$$-\det(\mathbf{\Sigma'}) \text{ minimum}$$

under **constraints**

$$\mathbf{U_1}(i) \mathbf{S_1}' \mathbf{S_1^T} \mathbf{U_1}(i)^{\mathrm{T}} \leq 1 \quad \forall i \in \{1, \ldots, m\}$$

The eigenvalues decomposition of $\mathbf{\Sigma'}$ leads to matrix $\mathbf{R'}$ and $\mathbf{D'}$. Matrix $\mathbf{X'} = \mathbf{R'D'}$ characterizes the linear application that transforms a unitary circle in the ellipse of maximum surface included into the operational polytop. The ratio of extreme diagonal values of $\mathbf{D'}$ constitutes the isotropy index built previously.

One can see that $\mathbf{X} = \mathbf{X'}$, that is to say that the ellipses obtained with both methods are the same. In fact referring to the definitions $\mathbf{X}$ of $\mathbf{X'}$ and, it can be verified that:

$$\mathbf{\Sigma} = \mathbf{S_1 X X^T S_1^T}, \tag{47}$$

$$\mathbf{\Sigma'} = \mathbf{X' X'^T}. \tag{48}$$

So the admissible domains constraints can be written as:

– Reasoning in joint space:

$$\mathbf{U_1}(i) \mathbf{S_1 X} \ \mathbf{X^T S_1^T} \mathbf{U_1}(i)^{\mathrm{T}} \leq 1, \tag{49}$$

– Reasoning in operational space:

$$\mathbf{U_1}(i) \mathbf{S_1 X X'^T S_1^T} \mathbf{U_1}(i)^{\mathrm{T}} \leq 1. \tag{50}$$

In joint space, $-\det(\mathbf{\Sigma})$ has to be minimized, that is $-\det(\mathbf{X X^T})$, because:

$$-\det(\mathbf{\Sigma}) = -2 \det(\mathbf{S_1}) \det(\mathbf{X X^T}), \tag{51}$$

$$\det(\mathbf{S_1}) > 0. \tag{52}$$

In operational space $-\det(\mathbf{\Sigma'})$ has to be minimized, that is: $-\det(\mathbf{X' X'^T})$. Thus, both entities are obtained as results of the same optimization problem under the same constraints.

## 5. DETERMINATION OF EXTREME VELOCITIES OF THE OPERATIONAL POLYTOP

In this section, the extreme velocities of the operational polytop will be determined. The "lowest" velocity is defined as the minimum velocity always reachable by the moving platform in all directions of the operational space. The "highest" velocity is the maximum velocity that can be reached by the moving platform in a very particular direction.

The highest velocity belongs necessarily to a vertex of the polytop; the lowest value is located on one of the faces (cf. Figure 15).

### 5.1 Finding $v_{polytop}^{max}$

Referring to Equation (44), a point $K'_i$ belonging to the $i^{th}$ face can be described by:

$$\mathbf{E_i^T S_1 K'_i} = 1 \tag{53}$$

a point $K'_{m+i}$, $i \in \{1, \ldots, m\}$, belonging to the adjacent face (the $(m+i)$th face) can be described by:

$$-\mathbf{E_i^T S_1 K'_{m+i}} = 1. \tag{54}$$

In the optimization problem faces of type (54) have not been considered; here they must be taken into account. A vertex of the polytop is a point of the $n$-dimensional operational space. The $2m$ frontier equations ($m$ of type (53) and $m$ of type (54)) will be seek, to find all the combinations of $n$ faces which generate a vertex. For this, all $C_{2m}^n$ possible systems will be seeked.

If the $i^{th}$ system can be solved, the fact that point $K'_i$, $i \in \{1, \ldots, 2m\}$ belongs to the polytop will have to be verified. The system might have no solution, for example when two vectors $\vec{e}_i$ and $\vec{e}_j$ have the same projection in the range of $\mathbf{J_m}$: $\mathbf{E_i} = \mathbf{E_j}$. Moreover, when a point $K'_i$ is established, this point might be located outside the admissible space (cf. Figure 19).

Once all vertices are determined, the highest distance between the center and points $K'_i$ is given by:

$$v_{parrallelogram}^{max} = \max_{i \in \{1, \ldots, 2m\}} \| \mathbf{K'_i} \| \tag{55}$$

### 5.2 Finding $v_{polytop}^{min}$

The lowest distance $v_{polytop}^{min}$ is measured between the center and a point located on one of the side of the polytop. Let us note $H'_i$ the closest point on side $i$. $OH'_i$ is collinear with the normal of this side.
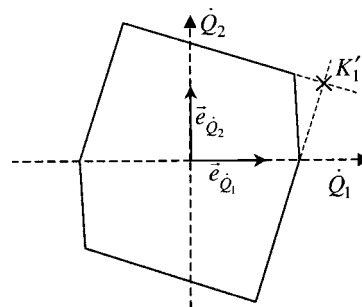


Fig. 19. Determination of a point outside from the admissable polytop.

Relation (53) for $H'_i$ and $i^{\text{th}}$ face is the following:

$$\mathbf{E}'_{\mathbf{i}}\mathbf{H}' = 1, \tag{56}$$

where $\mathbf{E}'_{\mathbf{i}} = \mathbf{S}_1 \mathbf{E}_{\mathbf{i}}$ is the normal vector to the side.

The collinearity relation can be written as follows:

$$\exists k / \mathbf{H}'_{\mathbf{i}} = k\mathbf{E}'_{\mathbf{i}}, \tag{57}$$

so, combining (57) and (56) implies:

$$\mathbf{E}'^{\mathrm{T}}_{\mathbf{i}} k\mathbf{E}'_{\mathbf{i}} = 1. \tag{58}.$$

Thus $k$ is:

$$k = 1 / \| \mathbf{E}'_{\mathbf{i}} \|^2. \tag{59}$$

By replacing the value of $k$ in relation (57) and by calculating the distance from point $H'_i$, $i \in \{1, \ldots, m\}$ to the center, this leads to:

$$\| \mathbf{H}'_{\mathbf{i}} \| = 1 / \| \mathbf{E}'_{\mathbf{i}} \|, \tag{60}$$

that is to say, by using expression of $\mathbf{E}'_{\mathbf{i}}$:

$$\| \mathbf{H}'_{\mathbf{i}} \| = 1 / \| \mathbf{S}_1 \mathbf{E}_{\mathbf{i}} \|. \tag{61}$$

Then, the sought value is given by:

$$v^{\min}_{parallelogram} = \min_{i \in \{1, \ldots, m\}} \| \mathbf{H}'_{\mathbf{i}} \|. \tag{62}$$

## 6. CONCLUSION

In this paper we have firstly shown the limits of classical analysis and indices simply based on the Jacobian matrix when Parallel Mechanisms with Actuation Redundancy are analyzed in terms of velocity isotropy. We have introduced new tools to analyze and optimize such mechanisms by considering their actual capabilities in task space instead of the quality of the velocity mapping. The first set of tools offers measures based on a classical point of view, a velocity ellipsoid, with an important feature: the sought ellipsoid is much closer to the real machine capability than the one usually considered. The second set of tools is based on the velocity polytop: the ways to efficiently compute such a polytop and, more important, its extreme values have been described. It is expected that indices based on both analysis can be usefully implemented in optimization processes for new redundant parallel mechanisms.

## References

1. J.K. Salisbury and J.J Craig, "Articulated hands: Force control and kinematic issues", *Int. J. Robotics Research* **1**(1), 4–17 (1982).
2. T. Yoshikawa, "Manipulability of robotic mechanisms", *Proc. Robotics Research: The Second International Symposium* (eds. H. Hanafusa and H. Inoue) (MIT Press, Cambridge (MA), USA, 1985) **Vol. 4**, pp. 3–9.
3. T. Yoshikawa, "Dynamic manipulability of robot manipulators", *Journal of Robotic Systems* **2**(1), 113–124 (1985).
4. C. Gosselin, "Dexterity indices for planar and spatial robotic manipulators", *Proc. IEEE ICR&A* (1990), pp. 650–655.
5. J. Angeles, "The design of isotropic manipulator architectures in the presence of redundancies", *Int. J. Robotics Research* **11**(3), 196–201 (1992).
6. C. Klein and T. Miklos, "Spatial robotics isotropy", *Int. J. Robotics Research* **10**(4), 426–437 (1991).
7. C. Gosselin and J. Angeles, "The optimum kinematic design of a planar three-degree-of-freedom parallel manipulator",

*ASME J. Mech., Trans., and Automation in Design* **110**, 35–41 (1988).
8. K. Zanganeh and J. Angeles, "Kinematic isotropy and the optimum design of parallel manipulators", *Int. J. Robotics Research* **16**(2), 185–197 (1997).
9. P. Chiacchio, S. Chiaverini, L. Sciavicco and B. Siciliano, "Global task space manipulability ellipsoids for multiple-arm systems", *IEEE Trans. On Robotics and Automation* **7**(5), 678–685 (1991).
10. A. Bicchi, C. Melchiorri and D. Balluchi, "On the mobility and manipulability of general limb robots", *IEEE Trans. On Robotics and Automation* **11**(2), 215–228 (1995).
11. F.C. Park and J.W. Kim, "Manipulability of Closed Kinematic Chains", *Recent Advances in Robot Kinematics* (eds. J. Lenarcic and V. Parenti-Castelli) (Kluwer, Dordrecht, 1996), pp. 99–108.
12. F. Marquet, S. Krut, O. Company and F. Pierrot, "Archi, a redundant mechanism for machining with unlimited rotation capacities", *Proc. of ICAR* (Budapest, August 2001).
13. S.J. Ryu, J.W. Kim, J.C. Hwang, C. Park, H.S. Ho, K. Lee, Y. Lee, U. Cornel, F.C. Park and J. Kim, "ECLIPSE: An Overactuated Parallel Mechanism for Rapid Machining", *Proc. ASME Int. Mechanical Engineering Congress and Exposition, USA* **8**, 681–689 (1998).
14. F. Pierrot and P. Chiacchio, "Evaluation of Velocity Capabilities for Redundant Parallel Robots", *Proc. of IEEE ICR&A* (Albuquerque, New Mexico, April 1997).
15. S. Kock and W. Schumacher, "A Parallel x-y Manipulator with Actuation Redundancy for High-Speed And Active-Stiffness Applications", *Proc. of IEEE ICR&A* (Leuven, Belgium, May 1998).
16. V. Hayward, O. Khatib, J. Craig and T. Lozano-Perez, "Kinematic Analysis And Design Of Redundant Manipulators", *Robotics Review 2*, (MIT Press, 1992), pp. 191–195.
17. L. Stocco, S. E. Salcudean and F. Sassani, "Matrix Normalization for Optimal Robot Design", *Proc. of IEEE ICR&A* (Leuven, Belgium, May 16–21, 1998).
18. V.C. Klema and A.J. Laub, "The singular value decompostion: its computation and some applications," *IEEE Transactions and Automatic Control* **AC-25**(2), 164–176 (1980).

## APPENDIX

### INFORMATION ABOUT "MANIPULABILITY OF CLOSED KINEMATIC CHAINS" BY PARK ET AL.[11]

A machine with closed kinematic chains is analyzed according the following notations:

- A set of $m$ joints whose positions $(q_1 \ldots q_m)$ describe the mechanism posture,
- The mechanism is composed of a total of $k$ joints (actuated or not); there positions are described by $(q_1 \ldots q_m \, q_{m+1} \ldots q_k)$,
- There are $p$ kinematic loops constraints (in space: $6p = k - m$, in plane: $3p = k - m$).

The principal axes of the manipulability ellipsoid are determined from the eigenvalues and eigenvectors of $\mathbf{M} = \mathbf{F}\,\mathbf{G}^{-1}\mathbf{F}^{\mathbf{T}}\mathbf{H}$, where:

- $\mathbf{F}$ is a matrix mapping the vector of velocities of joints (ranging from 1 to $m$) to $\mathbf{v}$, the velocity of the traveling plate, $\mathbf{v} = \mathbf{F}\,[\dot{q}_1 \ldots \dot{q}_m]^{\mathrm{T}}$,
- $\mathbf{H}$ is the task space metric (when position only is considered, $\mathbf{H} = \mathbf{I}$),

- $\mathbf{G} = \left[\dfrac{\mathbf{I_{m \times m}}}{-\mathbf{P}^{-1}\mathbf{A}}\right]^{\mathrm{T}} \mathbf{E} \left[\dfrac{\mathbf{I_{m \times m}}}{-\mathbf{P}^{-1}\mathbf{A}}\right]$ is the joint space metric

  ($\mathbf{E}$ is the metric on $\mathfrak{R}^k$, $\mathbf{E} = \mathbf{diag}(\varepsilon_1 \ldots \varepsilon_k)$, where $\varepsilon_i = 0$ for a passive joint, and $\varepsilon_i$ is proportional to the $i^{\mathrm{th}}$ motor capacity for an actuated joint).

To compute $\mathbf{P}$ and $\mathbf{A}$, the $i^{\mathrm{th}}$ kinematic constraint is written as the forward kinematics of an open chain with its end-effector fixed and stationary, and the associated Jacobian is derived as follows:

$$0 = \mathbf{A_i}\begin{bmatrix} \dot{q}_1 \\ \vdots \\ \dot{q}_m \end{bmatrix} + \mathbf{P_i}\begin{bmatrix} \dot{q}_{m+1} \\ \vdots \\ \dot{q}_k \end{bmatrix}, \; i = \{1, \ldots, p\}$$

Then the $p$ equations are stacked into a single equation:

$$0 = \begin{bmatrix} \mathbf{A}_1 \\ \vdots \\ \mathbf{A}_p \end{bmatrix}\begin{bmatrix} \dot{q}_1 \\ \vdots \\ \dot{q}_m \end{bmatrix} + \begin{bmatrix} \mathbf{P}_1 \\ \vdots \\ \mathbf{P}_p \end{bmatrix}\begin{bmatrix} \dot{q}_{m+1} \\ \vdots \\ \dot{q}_k \end{bmatrix} = \mathbf{A}\begin{bmatrix} \dot{q}_1 \\ \vdots \\ \dot{q}_m \end{bmatrix} + \mathbf{P}\begin{bmatrix} \ddot{q}_{m+1} \\ \vdots \\ \dot{q}_k \end{bmatrix}$$

*In the case study of section 2.3:*

- See Figure 20 for numbering of joints.
- $\mathbf{F} = \mathbf{I}$ and $\mathbf{H} = \mathbf{I}$; thus the matrix to be considered is simply: $\mathbf{M} = \mathbf{G}^{-1}$.
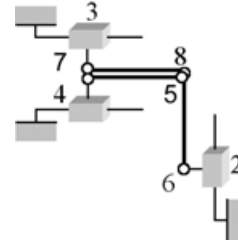


Fig. 20. Geometry of a specific PMAR (numbering of joints).

- Considering that all actuators have a maximum velocity of 1: $\mathbf{E} = \mathbf{diag}(1\;1\;1\;0\;0\;0\;0\;0)$

- $0 = \begin{bmatrix} 1 & 0 \\ 0 & 1 \\ 0 & 0 \\ 0 & 0 \\ 0 & 1 \\ 0 & 0 \end{bmatrix}\begin{bmatrix} \dot{q}_1 \\ \dot{q}_2 \end{bmatrix} + \begin{bmatrix} 0 & l & l & 0 & 0 & 0 \\ 0 & l & 0 & 0 & 0 & 0 \\ 0 & 1 & 1 & 1 & 0 & 0 \\ 1 & l & l & 0 & 0 & 0 \\ 0 & 0 & 0 & 0 & l & 0 \\ 0 & 0 & 0 & 1 & 1 & 1 \end{bmatrix}\begin{bmatrix} \dot{q}_3 \\ \dot{q}_4 \\ \dot{q}_5 \\ \dot{q}_6 \\ \dot{q}_7 \\ \dot{q}_8 \end{bmatrix}$

- Thus: $\mathbf{G} = \begin{bmatrix} 2 & 0 \\ 0 & 1 \end{bmatrix}$ and $\mathbf{M} = \begin{bmatrix} 1/2 & 0 \\ 0 & 1 \end{bmatrix}$.